NUMERICAL MODELING OF MOISTURE TRANSFER IN THE STRUCTURES OF A NEAR-SURFACE RADIOACTIVE WASTE DISPOSAL FACILITY

Anisimov N. A., Kuvaev A. A.

FSBI Hydrospetzgeologiya, Moscow, Russia

Article received on August 2, 2022

The paper considers a model used to calculate the flow in the structural elements of a near-surface radioactive waste disposal facility (RWDF). It presents the results of calculations focused on the flow and moisture field rates inside the RWDF taking into account changes in the properties of the upper cap, concrete and packages with radioactive waste occurring over time. The study also analyzes the influence of the flow field features on the safety barriers state.

Keywords: *radioactive waste, RWDF structures, safety barriers, radioactive waste packages, degradation, flow, moisture content, rainfall drainage.*

Introduction

RW repository designs provide for a system of safety barriers. Their main function is seen in preventing nuclide release into the environment or reducing its rate to an acceptable level.

Radionuclide release beyond near-surface disposal facilities (NSDF) is mainly driven by seepage water flows occurring due to the ingress of atmospheric precipitation and groundwater flows. In this regard, water flows occurring in the NSDF structures shall be calculated and predicted considering the properties of repository materials changing over time, which is seen as an important task of the safety assessments.

Experience of the Federal State Budgetary Institution Hydrospetzgeologiya shows that it's feasible to develop groundwater flow and transport models for the repository near and far fields separately from the NSDF model with the repository itself viewed as a potential source of radionuclide release into groundwater, which is explained by its small scale compared to the regional one. At the same time, both NSDF and regional groundwater flow models shall be coupled through the near field. Practice shows that the use of standard hydrogeological modeling tools such as MODFLOW [1] in the development of NSDF models appears to be quite impracticable due to their inherent features geared to the geological environment with multiple features characterizing the flow structure, primarily referring to the stratification of water-bearing sediments. Moreover, computational mesh generation is seen as another challenging aspect driven by the complexity of NSDF designs.

Given this circumstance, universal software tools designed for multiple physics modeling may come forward to address numerical analysis of processes occurring in NSDF, in particular, the COMSOL Multiphysics [2]. Its capabilities are discussed below based on a case study exploring a groundwater flow model developed for a NSDF

NSDF designs and calculation model geometry

Disposal facilities intended for Class 3 and 4 RW available or being developed in Russia are mainly near-surface type repositories. A calculation model prototype is discussed below based on the NSDF design developed for the SCC site [3, 4].

This structure having an elongated shape (186 × 24 m) involves 12 compartments (Figure 1). Figure 2 shows the compartment structure presented as a vertical section going along the a—a line.

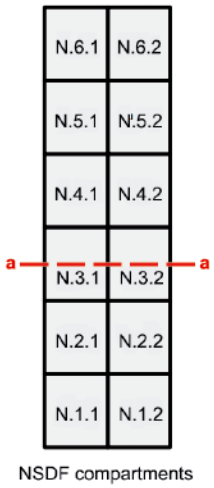

Figure 1. Layout of disposal compartments within the near-surface repository structure

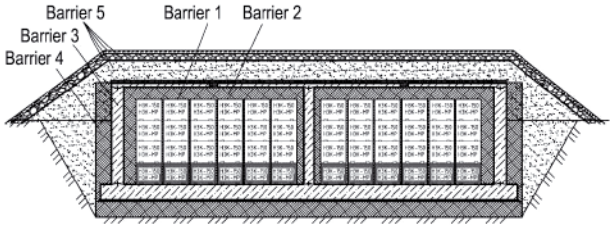

Figure 2. Design of NSDF compartments [3, 4]

Figure 2 presents the engineered safety barriers (EB 1 – EB 5), in particular:

Barrier 1 (EB 1): walls of a RW package.

Barrier 2 (EB 2): buffer material (clay powder) filling the gaps between the packages and the space between the packages and the inner compartment surfaces that remained empty after the compartment was loaded with RW packages. The size of gaps backfilled with buffer material depends on the RW package dimensions.

Barrier 3 (EB 3): bentonite walls — 800 mm, bottom slab — 1,000 mm, upper slab — 250 mm.

Barrier 4 (EB 4): clay retainer installed along the perimeter of the structure (walls, bottom) — 1,000 mm.

Barrier 5 (EB 5): multilayer covering cap constituting of the following layers (from the top to the bottom):

- soil-vegetative layer — 200 mm;
- drainage layer — 420 mm;
- bentomat (1st layer) — 30 mm;
- a layer of compacted clay or loam — 1,170 mm;
- sand — 200 mm;
- bentomat (2nd layer) — 30 mm.

Geometry of the computational model has been based on the NSDF compartment designs shown in Figure 2 involving the above safety barriers. Unlike the prototype, a gable shape of the upper slab has been specified in the model instead of a flat one, which is also commonly applied in these designs [3]. According to NSDF designs, packages with Class 4 RW are placed on the top of RW Class 3 packages. The calculation model assumes that Class 4 waste packaged into metal containers is stacked in the top three tiers, Class 3 waste packaged into reinforced concrete containers is disposed of in the bottom tier. Their dimensions are set according to those of the KMZ and NZK-150 containers [5]; 100 mm-wide gaps were proposed between the containers.

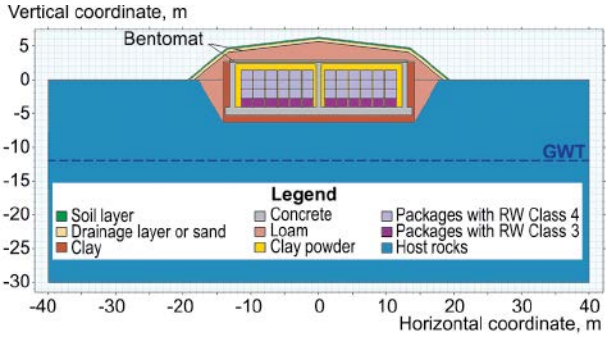

Figure 3. Geometry of the calculation model

Figure 3 presents the geometry adopted in the model with relevant safety barrier materials being indicated. The model also specifies the near field of the host rocks (80 × 30 m) and the groundwater table (GWT). The near field characteristics have been specified based on the surveys implemented at a real-life object. The water-bearing deposits of the near field involve loams, whereas the average annual depth of the groundwater level amounts to 12 m from the earth's surface.

Calculation model

For simplification purposes and considering that the longitudinal NSDF dimension essentially predominates over the transverse one, a two-dimensional (profile) setting was applied in the simulations (the calculated profile goes across the structure — Figure 1, section a—a).

To calculate moisture flow in a porous medium, the Richards equation is used if recharge-discharge points are absent [6]:

$$\frac{\partial\theta(h)}{\partial t}=\frac{\partial}{\partial x_i}\left[k_w(h)\left(K_{ij}\frac{\partial h}{\partial x_j}+K_{iz}\right)\right], \quad (1)$$

where:

$$k_w(h)=kS_e^l\left[1-\left(1-S_e^{1/m}\right)^m\right]^2,\ m=1-\frac{1}{n},\ n>1, \quad (2)$$

$$S_e=\frac{\theta-\theta_r}{\theta_s-\theta_r}=\frac{1}{\left[1+|\alpha h|^n\right]^m}, \quad (3)$$

where: θ is the current volumetric moisture content of the rocks, θ_r is the maximum volumetric content of bound water, θ_s is the total volumetric moisture content of the rocks, S_e is the relative moisture content, t is time (days), k_w is the moisture flow coefficient (m/day), k is the flow coefficient at full moisture saturation (m/day), h is suction head (m), x_i ($i=1, 2$) are spatial coordinates (m), K_{ij} is unit matrix, α, n are Van Genuchten parameters, l is the tortuosity parameter for pore channels. Double index ij means summation over all possible combinations.

It was further assumed that x_1 corresponds to the horizontal coordinate, and x_2 — to the vertical one. Therefore, K_{iz} stands for a value being equal to zero for $i=1$ and equal to 1 for $i=2$.

NSDF structures involve materials the properties of which have been identified based on preliminary R&D performed at the design development stage [7, 8]. In this case, if calculations are based on equation (1), relevant parameters are set according to the averaged reference hydraulic properties of the safety barrier materials in accordance with [9—11]. Table 1 summarizes these parameters and their values.

Table 1. Hydraulic properties of soils and materials

Soils and materials	k, m/day	θ_s	θ_r	α, 1/m	n	l
Coarse/fine sand	1.30/ 0.28	0.442	0.05	2.924	2.094	0.5
Loams constituting to the host rocks/caps	0.02/ 0.01	0.525	0.096	1.9	1.31	0.5
Clay	5e–5	0.542	0.071	1.28	1.276	0.5
Soil-vegetable layer	0.3	0.7	0.2	1.9*	1.31*	0.5
Bentonite (clay powder)	4.3e–6	0.542***	0.071***	1.28**	1.276**	0.5
Degraded/non-degraded concrete***	8.6e–8/ 0.28	0.15/ 0.442	0.1/ 0.05	1.28*/ 2.924	1.276**/ 2.094	0.5

Notes:
* according to the value set for loams;
** according to the value set for clay;
*** according to the value set for fine sand

Since no data were available in the literature sources, some soil, vegetable soil, bentonite and concrete characteristics in Table 1 were set equal to those of materials with most similar properties: sand, loam and clay.

Figure 4 schematically presents the boundary conditions for a flow model, namely, for the NSDF and part of its near field.

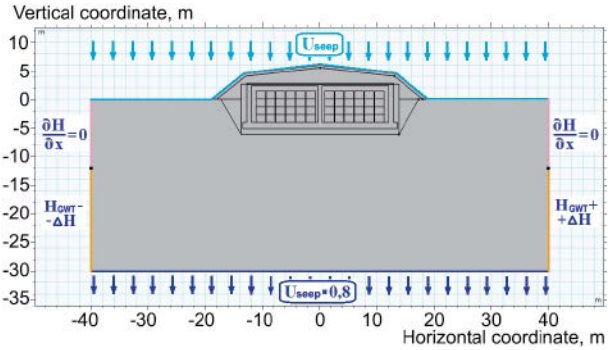

Figure 4. Schematical representation of boundary conditions for a flow model

The following boundary conditions were set:

- at the top boundary — the groundwater seepage recharge module: U_{seep};
- at the bottom boundary — groundwater outflow rate calculated based on the following expression: $U_{seep}\times 0.8$ (based on calculations performed using the regional model);
- on the right and left boundaries from the GWT and downwards — piezometric head, respectively: $H_{GWT}+\Delta H$ and $H_{GWT}-\Delta H$;
- on the right and left boundaries above the groundwater table — an impenetrable boundary: $\partial H/\partial x=0$.

The boundary conditions for local NSDF site areas are usually set based on the regional model calculations. In this case, they correspond to the average conditions characteristic for the repository site [4]. Seepage recharge module (W_{seep}) was set equal to 0.05 m/year. The initial GWT position was set at a depth of 12 m: $H_{GWT}=-12$ m. ΔH specifying the difference between the groundwater levels changing lateralward was set according to the regional model - 0.8 m.

The service life of engineered barriers represented by concrete building structures and container walls is limited. It was assumed that initially the hydraulic properties of these elements would correspond to concrete and after complete degradation they would acquire the properties of a fine-grained sand (Table 1). Property changes occurring between these states are characterized with a time dependency resulting from chemical transformations driven by water flows through concrete, mechanical loads and microbiological effects [11]. Figure 5

exemplifies this aspect using a time dependency showing fluctuations in concrete properties along with the damage growing due to chemical and mechanical impacts [12].

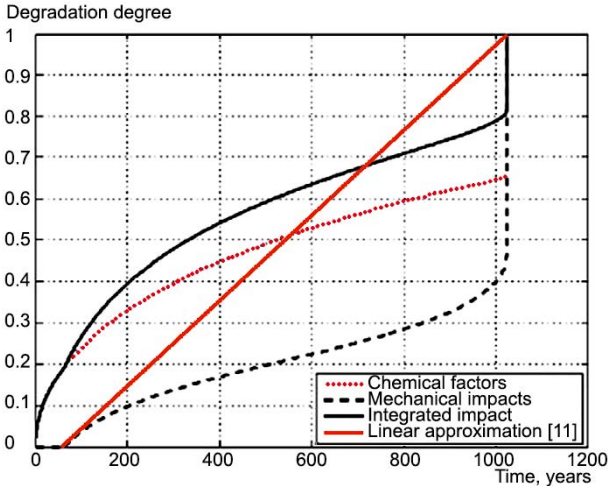

Figure 5. Damage accumulated in concrete due to chemical and mechanical impacts [12]

Figure 5 also shows a linear dependence for the changing properties of concrete structures, which is a simplifying approximation. It is used to address practical problems in NSDF safety assessments discussed in [11].

However, based on a linear dependency, one cannot interpolate the values differing by several orders of magnitude, in particular, the flow coefficient for concrete before and after its degradation. Therefore, exponential function is used in the calculations:

$$a(t)=\begin{cases} a_1 & t<t_1 \\ a_1\left(\frac{a_2}{a_1}\right)^{\frac{t-t_1}{t_2-t_1}} & t_1\le t\le t_2 \\ a_2 & t_2<t \end{cases} \qquad (5)$$

This function provides a linear approximation given relatively equal values a_1 and a_2 and a smooth transition in case of a big difference. In the calculation model, this function sets the changes in the hydraulic properties occurring during the degradation of NSDF compartment elements, including concrete structures, bentomats and RW packaging material.

Table 2 presents the time when the degradation process taking place in the NSDF compartment elements starts (t_1) and gets completed (t_2) assumed in the calculations. They are set according to the diagrams showing the changing properties of the safety barriers used in [11].

Table 2. Periods of safety barrier degradation

NSDF compartment element	Degradation starts (t_1), years	Degradation completed (t_2), years
Concrete walls and foundation	50	1,000
Concrete slab	50	300
Bentomat	100	500
Packages with RW Class 3	200	400
Packages with RW Class 4	0	100

The calculation model was built and the calculations were performed based on the finite element method implemented in the COMSOL Multiphysics software [2]. The breakdown into computational cells was carried out using an irregular triangle mesh. The total number of the cells amounted to over 160 thousand. Figure 6 presents a fragment of such breakdown into computational cells.

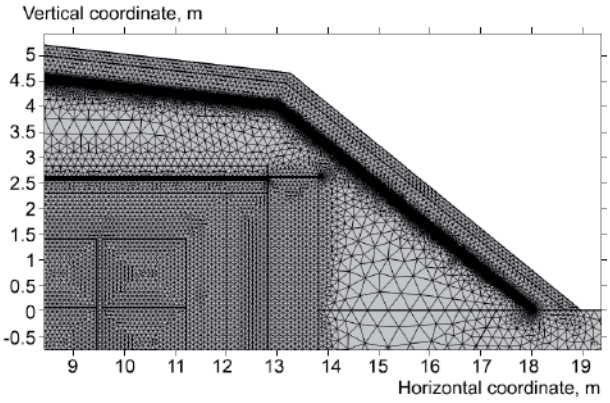

Figure 6. Model breakdown into computational cells (fragment)

The developed model covers a time interval from 0 to 1,000 years. Figures 7a—7c show the flow rate fields calculated for three timepoints, namely, 0, 100, and 1000 years.

Figures 7a—7c reflect the stages of flow formation in NSDF structural elements and RW packages. At the initial timepoint (0 years), flow resistance of concrete structures and RW packages is the highest. Therefore, the rate of flows passing through them is relatively low. According to the assumed conditions, degradation of packages with RW Class 4 is believed to be completed after 100 years, therefore, the rate of flows passing through them is expected to get much higher, thereby, affecting the packages with RW Class 3 (Figure 7b).

The flow rate field shown in Figure 7c corresponds to a timepoint of 1,000 years: by this time, safety barrier degradation is expected to be completed.

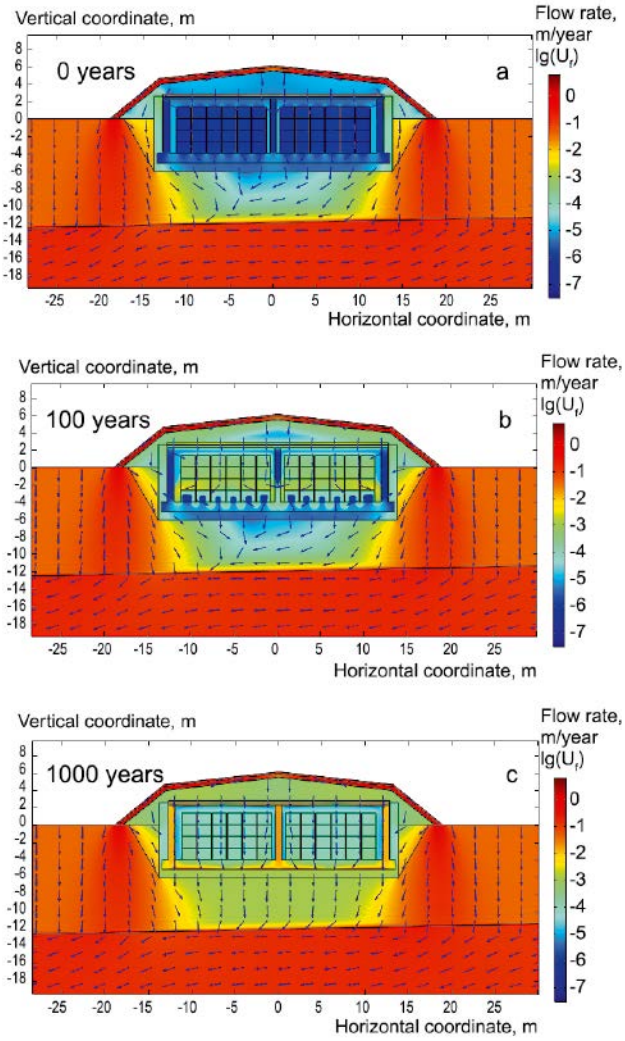

Figure 7. Filtration rate fields in NSDF structural elements and RW packages calculated for three timepoints: 0 (a), 100 (b) and 1,000 years (c)

Concrete walls and foundation would become conductive "channels" providing low seepage resistance. The flow will basically pass along them bypassing the area with RW packages and bentonite clay backfill. Figure 8 provides a detailed picture of flows, namely of their vectors and rates at a timepoint of 1,000 years.

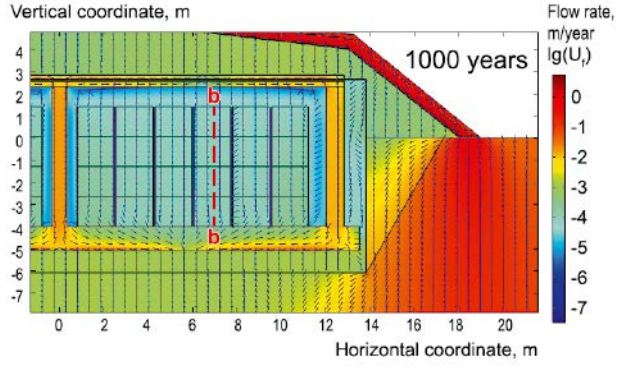

Figure 8. Flow rate fields in the repository siting area at a timepoint of 1,000 years (b—b – flow rate profile)

The intensity of radionuclide release from NSDF compartments depends on the flow rate in the RW packages. At the initial timepoint, the flow rates in the RW disposal area are very low amounting to some 10^{-6}—10^{-8} m/year. Over time, hydraulic properties of the packaging materials alter due to degradation processes, active porosity increases causing moisture release out of these materials and its transport from the top RW layers to the bottom ones.

All along RW package degradation process from its start till its completion, which corresponds to a time interval of up to 400 years (Table 2), the flow rate field in the disposal area is expected to be highly heterogenous. Then it is expected to become homogenous. After 1,000 years, redistribution of moisture accumulated in the structural repository elements and RW packages is expected to be completed. After that, the flow rate in the RW disposal area is expected to drop to a certain level depending on the flow rate of atmospheric moisture seeping through the safety barriers that would no longer perform their safety functions.

Figure 9 shows the filtration rate fluctuations in the RW disposal area (along line b—b shown in Figure 8) considering different timepoints characterizing different stages of safety barrier degradation.

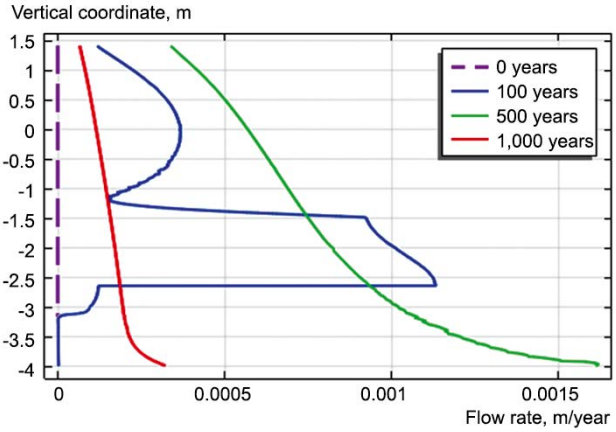

Figure 9. Plots of filtration rates along the height of the RW disposal area at the timepoints of 0, 100, 500 and 1000 years

The flow rate profile established after the transient processes associated with the safety barrier degradation are completed, which corresponds to a time period of 1,000 years (Figure 9), is characterized by an increased flow from the top tier of RW packages to the bottom one. Thus, the bottom tier of RW packages is exposed to least favorable conditions involving more intense flows. In this regard, if one changes the layout of RW packages in the repository compartment so that the packages

with RW Class 4 constitute to the bottom tier with RW Class 3 packages placed above them, this would decrease the level of radionuclide leaching and, in the long term, reduce the radionuclide release from the repository compartment to the geological environment.

Moisture characteristics of repository structures

The calculations assumed that the clay retainer and backfill material (moistened clay powder) do not have gaps and remain continuous throughout the entire modeling period. However, due to mechanical loads, for example, in case of a seismic impact, these barriers may lose their integrity. Whether the cracks that have evolved in the clay remain unsealed or get sealed quickly depends on the plasticity level of the clay, which, in turn, is governed by its moisture content.

Figure 10 presents relative moisture content S_e (3) calculated for the repository elements and the near-field host rocks. At the initial timepoint (0 years), the moisture distribution was calculated assuming a steady initial state of the safety barriers. According to the simulation results, RW packages and concrete structures are characterized by most substantial transformations as regards this indicator during their degradation. This phenomenon is explained by a decreased capillary rise [13] caused by the leaching of binding components found in the concrete and the matrix material.

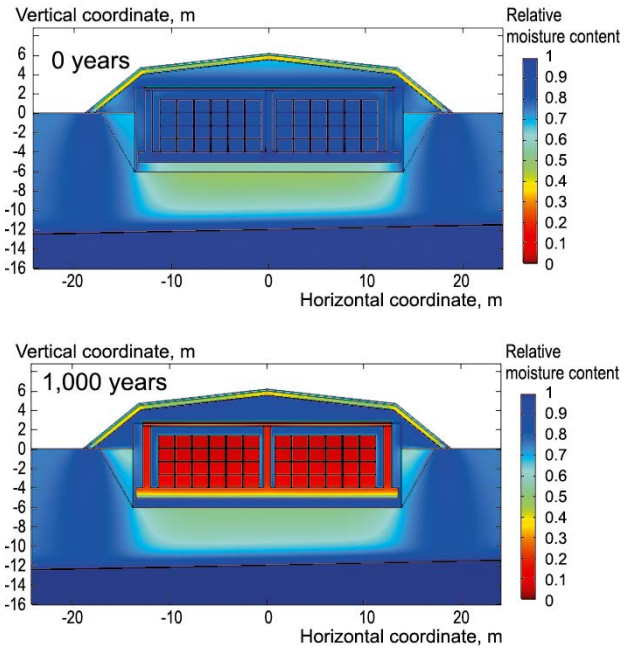

Figure 10. Calculated relative moisture content in the repository elements and host rocks of the near field within a time period from 0 to 1,000 years

Relative moisture content of the clay retainer and bentonite backfill changes to a lesser extent, which is shown in Figure 11.

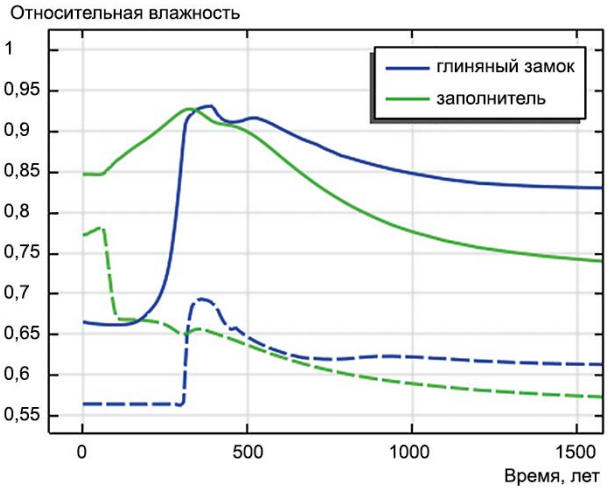

Figure 11. Fluctuations of the averaged (solid line) and minimum (dotted line) relative moisture content levels for the clay retainer and bentonite backfill materials

Minimum relative moisture content levels for the entire simulation time are as follows:

- for the clay retainer: 0.56;
- for the bentonite backfill: 0.57.

At these relative moisture content levels, the clays remaining in the natural state may have the properties of a solid material, and those characterized with a disturbed structure, which include clays constituting to the repository safety barriers, appear to be plastic [14]. In this regard, given such repository designs and the hydrogeological conditions, only a short-term discontinuity of clay materials may arise. In general, they are expected to perform the required barrier functions over long periods of time.

Drainage of atmospheric precipitation

Figures 7a—7c show that a significant proportion of atmospheric precipitation is discharged towards the periphery of the structure due to the drainage layer and the inclination of the upper cap. A parametric study was performed to evaluate the dependency between the angle of the upper slab inclination and the amount of precipitation seeping below the drainage layer. Under the study, a series of calculations was run, which has required some model geometry upgrading. Table 3 presents the calculated proportions of precipitation seeping beneath the drainage layer.

According to Table 3, moisture flow penetrating beneath the drainage layer depends on the angle of

Table 3. Calculated proportions of atmospheric precipitation seeping under the drainage layer

Inclination angle of the cap, °	Portion of precipitations seeping under the cap, %		Increased portion of precipitation after 1,000 years, %
	0 years	After 1,000 years	
0	7.75	7.95	2.56
4	5.65	5.84	3.44
8	4.67	4.74	1.59
12	4.03	4.06	0.94
16	3.5	3.53	0.96
20	3.02	3.03	0.43

the upper cap inclination ranging from 3 to 8 %. Its increase from 0 to 20 ° results in almost 3-fold decrease in the seepage amount. These values were compared for the timepoints of 0 and 1,000 years: it has been demonstrated that safety barrier degradation (concrete walls of the repository structure and additional safety barriers represented by bentomat layer) would result in a seepage flow intensification by no more than 3.5 %. Thus, clay retainer and a layer of compacted loam constituting to the upper cap shall be considered as the key barriers preventing moisture seepage below the drainage layer. Whereas bentomat introduction into repository designs produce no significant effect on the rate of flows seeping beneath the drainage layer.

Conclusion

The computational study based on a flow model built for a repository compartment has yielded following conclusions.

The rate of flows passing through the RW packages is heterogenous along the height of the package stack and increases towards the foundation of a repository compartment. In this regard, to reduce radionuclide flow into the host rocks, special layouts are introduced to the repository designs providing for RW Class 3 package installation above the compartment foundation. For example, RW Class 3 packages may be stacked in the second tier from the bottom, whereas those with RW Class 4 – in the first tier.

Moisture content was calculated for the clay retainer and backfill materials of a repository compartment. It was demonstrated that over the entire modeling interval, these materials were expected to retain their plastic properties, thereby the emerging cracks would get sealed. Thus, under external mechanical action, only short-term discontinuities are expected to occur in these materials and, in general, over long-term periods, they are expected to perform the required barrier functions.

Clay retainer together with the upper cap structure involving a drainage layer and a structure made of a low water permeability material are seen as the key barriers preventing the seepage of atmospheric precipitation into the repository. The moisture flow seeping beneath the drainage layer provided for in the repository designs accounts for some 3 – 8 % depending on the angle of the upper cap inclination.

Computational modeling implemented under this study showed that the flow rate mode occurring within the repository throughout the safety barrier degradation period had a quite complex spatial structure varying over time depending on a combination of various factors. Based on its study the repository designs may be optimized, thereby, enhancing the repository safety.

References

1. Chiang W., Kinzelbach W. 3D-Groundwater Modeling with PMWIN: A Simulation System for Modeling Groundwater Flow and Pollution. Springer, 2001.

2. Kovalenko A., Uzdenova A., Urtenov M., Nikonenko V. *Matematicheskoye modelirovaniye fiziko-khimicheskikh protsessov v srede COMSOL Multiphysics 5.2*. [Mathematical modeling of physical and chemical processes in COMSOL Multiphysics 5.2]. Saint-Petersburg, Lan Publ., 2017. 228 p.

3. Pavlov D. I., Sorokin V. T., Barinov A. S., Demin A. V., Sychenko D. V. Nauchno-tekhnicheskiye i proyektnyye osnovy sozdaniya konstruktsiy pripoverkhnostnykh punktov zakhoroneniya nizko- i sredneaktivnykh otkhodov [Scientific and Design Aspects in the Development of Near-Surface Disposal Facilities for Low- And Intermediate-Level Waste]. *Radioaktivnyye otkhody — Radioactive Waste,* 2021, no. 4 (17), pp. 65—77. DOI: 10.25283/2587-9707-2021-4-65-77.

4. License application materials for siting and construction of a near-surface disposal facility for solid radioactive waste Class 3 and 4, Tomsk Region, Seversk City District. Vol. 1. — Moscow, FSUE NO RAO Publ., 2018.

5. Gataullin R. M., Medelyayev I. A., Sharafutdinov R. B. Ispol'zovaniye perspektivnykh tekhnologiy dlya resheniya problem bezopasnogo obrashcheniya s radioaktivnymi otkhodami [Promising methods and their application in addressing the problems associated with the safe radioactive waste management]. *Yadernaya i radiatsionnaya bezopasnost' — Nuclear and Radiation Safety,* 2008, no. 4 (50), pp. 68—75.

6. Šimůnek J., van Genuchten M. Th., Šejna M. The HYDRUS Software Package for Simulating the Two- and Three-Dimensional Movement of Water, Heat, and Multiple Solutes in Variably-Saturated Porous Media. Technical manual. Version 3.0. Preprint Department of Environmental Sciences University of California Riverside. California, 2012. 260 p.
7. Pavlov D. I., Ilina O. A. O sistemnom podkhode k vyboru bar'yerov bezopasnosti dlya zakhoroneniya RAO klassov 3 i 4 [On a System Approach to the Selection of Safety Barriers for the Disposal of Radioactive Waste Class 3 and 4]. *Radioaktivnyye otkhody — Radioactive Waste,* 2020, no. 3 (12), pp. 54—65. DOI: 10.25283/2587-9707-2020-3-54-65.
8. Ilina O. A., Krupskaya V. V., Vinokurov S. E., Kalmykov S. N. Sovremennoye sostoyaniye v razrabotkakh i ispol'zovanii glinistykh materialov v kachestve inzhenernykh bar'yerov bezopasnosti na ob'yektakh konservatsii i zakhoroneniya RAO v Rossii [State-of-Art in the Development and Use of Clay Materials as Engineered Safety Barriers at Radioactive Waste Conservation and Disposal Facilities in Russia]. *Radioaktivnyye otkhody — Radioactive Waste,* 2019, no. 4 (9), pp. 71—84. DOI: 10.25283/2587-9707-2019-4-71-84.
9. Zhonghui Ou. Differential Evolution's Application to Estimation of Soil Water Retention Parameters. *Agronomy,* 2015, no. 5, pp. 464—475.
10. Expert system: Database of the IGE RAS. 2017.
11. ISAM. *Safety Assessment Methodologies for Near Surface Disposal Facilities.* V.1, 2. — IAEA, Vienna, 2004.
12. Bart F., Cau-dit-Coumes C., Frizon F., Lorente S. *Cement-Based Materials for Nuclear Waste Storage* / ISBN 978-1-4614-3445-0 (eBook). Springer Science+Business Media, New York, 2013.
13. Shein E. V. *Kurs fiziki pochv* [Soil physics course]. Moscow, Moscow State University Publ., 2005. 432 p.
14. Sergeev E. M., Golodkovskaya G. A., Ziangirov R. S. et al. *Gruntovedeniye* [Ground science]. Edt. by Member of the Academy of Science E. M. Sergeyev — Moscow, Moscow State University Publ., 1983. 392 p.

Information about the authors

Anisimov Nikolai Alexandrovich, chief specialist, FSBI "Hydrospetzgeologiya" (4, Marshal Rybalko st., Moscow, 123060, Russia), e-mail: anisn@msnr.ru.

Kuvaev Andrey Alekseevich, doctor of Geological and Mineralogical Sciences, head of department, FSBI "Hydrospetzgeologiya" (4, Marshal Rybalko st., Moscow, 123060, Russia), e-mail: kuvaev@msnr.ru.

Bibliographic description

Anisimov N. A., Kuvaev A. A. Numerical Modeling of Moisture Transfer in the Structures of a Near-Surface Radioactive Waste Disposal Facility. *Radioactive Waste,* 2022, no. 3 (20), pp. 97—106. DOI: 10.25283/2587-9707-2022-3-97-106. (In Russian).